

OPTIMIZATION OF a-SiGe BASED TRIPLE, TANDEM AND SINGLE-JUNCTION SOLAR CELLS

Xunming Deng

Department of Physics and Astronomy, University of Toledo, Toledo, Ohio 43606

ABSTRACT

Recent research activities at the University of Toledo (UT) in the fabrication of high-efficiency triple, tandem and single-junction solar cells, all employing high-quality a-SiGe cells, are reviewed in this paper. Incorporating various improvements in device fabrication, the UT group fabricated 1) triple-junction a-Si/a-SiGe/a-SiGe solar cells with 12.5% initial efficiency and 10.7% stable efficiency, tandem-junction a-Si/a-SiGe solar cells with 12.9% initial efficiency, and single-junction a-SiGe solar cells with 12.5-13% initial efficiency and 10.5% stable efficiency. This review also highlights recent UT work on the nanocrystalline silicon p-layer and light-assisted electrochemical shunt passivation process.

INTRODUCTION

This paper reviews some of the recent research activities related to a-Si based solar cells at the University of Toledo (UT). These a-Si based research activities are related to and in support of some of the previous efforts at Energy Conversion Devices, Inc and United Solar Ovonic Corp. [1-5]. The UT a-Si research effort started in 1996 and has since covered a broad range of activities, including fabrication, analysis and modeling of single, tandem and triple-junction a-SiGe based solar cells and materials [6-19]. Much of the research is also summarized in a recent report [20]. While there is extensive research activities and significant progress made worldwide in the related areas [21, 22], this paper is limited to a brief review of UT activities in a-Si based photovoltaics, which is centered around substrate-type, a-Si/a-SiGe/a-SiGe triple-junction solar cells deposited on thin stainless steel foil, having a structure shown in Figure 1.

EXPERIMENTAL

In the layers shown in Figure 1, the nine semiconductor layers (n-p-n-p-n) are deposited using a capacitively coupled plasma enhanced chemical vapor deposition (PECVD) system and the non-semiconductor layers (Ag, ZnO and ITO) are deposited using magnetron sputtering. Figure 2 shows the present nine-chamber PECVD/Sputtering cluster tool used at UT for the fabrication of triple-junction solar cells [19]. This system, with four PECVD chambers, four sputter chambers and one load-lock chamber, all connected together by gate valves, allows researchers at UT to fabricate all 12 layers of 4"x4" triple-junction solar cells without vacuum break. It

also allows the fabrication of up to ten 4"x4" devices each time or with up to nine masks that can be changed in situ without vacuum break [19]. The a-Si and a-SiGe i-layers are deposited using a gas mixture of Si₂H₆, GeH₄ and H₂ while the p- and n-layers are deposited using gas mixtures of SiH₄, BF₃ and H₂ and SiH₄, PH₃ and H₂, respectively, and at a pressure range of 0.6-1.0 Torr, as standard deposition conditions.

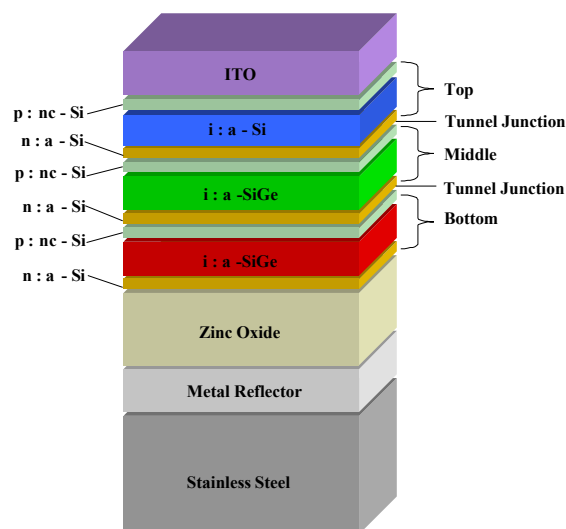


Fig. 1 Device structure of a-Si/a-SiGe/a-SiGe triple-junction solar cells used at UT.



Fig. 2 Photo of UT's 9-chamber solar cell fabrication system.

The solar cells fabricated are then evaluated using I-V measurement system under a solar simulator and quantum efficiency system having a bias light and bias voltage for the measurement of multiple-junction cells. Materials characterization using Raman, XRD, optical transmission, FTIR, dark and photo-conductivities, and SEM/TEM are routinely performed. Details about the fabrication and characterizations have been reported earlier [6-20].

RESULTS AND DISCUSSIONS

a-Si and a-SiGe i-layers

The intrinsic a-Si and a-SiGe layers are deposited using Si_2H_6 and GeH_4 with strong hydrogen dilution so that the structure of these materials are near the transition from amorphous to amorphous-microcrystalline mixed phase. The bandgaps for the top, middle and bottom component cells, with structure shown in Fig. 1, are approximately 1.85, 1.65 and 1.45 eV. The bandgap of the bottom a-SiGe cell is graded to enhance hole transport.

p-layer for wide bandgap a-Si top cell

The p-layer used for the wide bandgap a-Si top cells is deposited at a low temperature ($\sim 70 - 100^\circ\text{C}$), with a strong H dilution and at a high rf power. The p-layer material is a nanocrystalline Si (nc-Si) and a-Si mixed-phase material, having 3-5nm sized nc-Si grains, imbedded in a-Si matrix [11,16]. Figure 3 shows TEM micrographs of a 15nm thick nc-Si p-layer deposited on 15nm thick a-Si i-layer, to simulate the growth conditions and thickness of an actual p-layer. In the high-angle annular dark-field (HAADF) image shown in Fig. 3a, the bright dots represent nanocrystalline particles. The insert in Fig. 3a shows a selected-area electron diffraction (SAED) image, showing a diffraction pattern with crystalline feature for the area probed. Figure 3b shows a high-resolution electron microscopy (HREM) image, exhibiting the nanocrystalline lattice. Fig. 3c is a nano electron diffraction (NED) taken from one of the bright dots in Fig. 3a, indicating the crystalline nature of the particle. The interference fringes separated by 0.31nm correspond to the spacing of Si (111) planes of the nanocrystals. The bandgap of the nc-Si grains in the p-layer is believed to be enlarged due to quantum confinement effect (QCE), making it more suitable for wide bandgap a-Si top cells and resulting in high open circuit voltage for single-junction a-Si cells, with V_{oc} up to 1.04 V, as shown in Figure 4a [11,16]. Another sample, having a larger-grained microcrystalline silicon p-layer deposited at a higher temperature and a lower rf power while all of the other layers in the device are deposited under identical conditions as the samples shown in Figure 4a, exhibits a lower V_{oc} ($\sim 0.53\text{V}$).

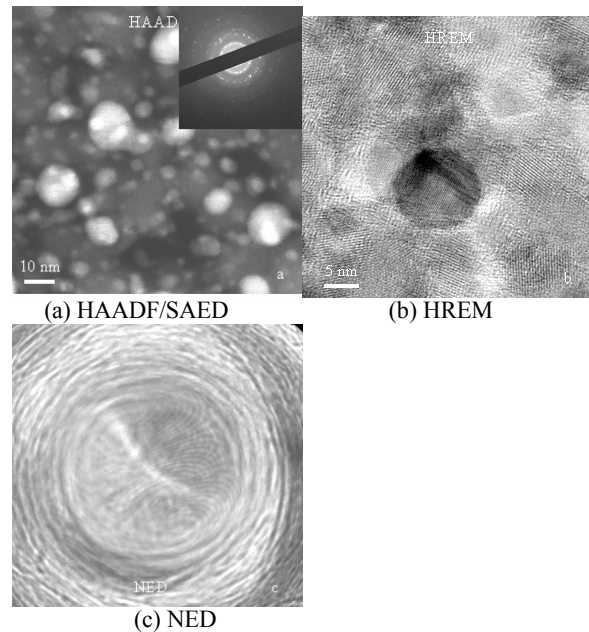


Fig. 3 TEM micrographs of a nc-Si p-layer.

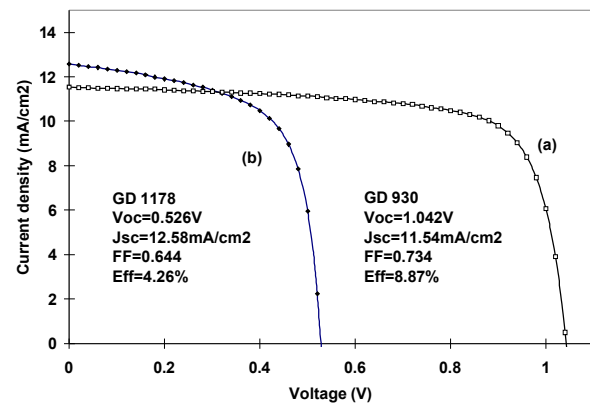


Fig. 4 IV curves of a wide bandgap a-Si solar cell having a nc-Si p-layer (a) and a $\mu\text{c-Si}$ p-layer (b), showing V_{oc} of 1.04V and 0.53V, respectively.

Tunnel-junctions

An important aspect in the optimization of multiple-junction solar cell fabrication is to have an improved tunnel/recombination junction layer between component cells. The multiple-junction a-Si solar cells at UT employ heavily doped thin interface layers, $\sim 1\text{nm}$ thick, deposited with doping gas ratios BF_3/SiH_4 and PH_3/SiH_4 of ~ 1 to 1.5, at the tunnel/recombination junctions to enhance carrier recombination thus reduce the series resistance and increase device fill factor [8]. Table 1 shows a series of triple cells incorporating heavily doped interface layers of different thicknesses. It is found that a 10 s deposition for the interface layers is optimal, with high V_{oc} and high FF.

Table 1 IV performance of triple cells having heavily doped interface layers at the tunnel/recombination junctions.

p ⁺ and n ⁺ interface layer deposit time (s)	V _{oc} (V)	J _{sc} (mA/cm ²)	FF (%)	η (%)	Device No.
p ₁ ⁺ & p ₂ ⁺ n ₂ ⁺ & n ₃ ⁺					
0	2.300	7.25	68.4	11.4	GD846
10	2.314	7.54	69.2	12.1	GD840
20	2.276	7.55	69.7	11.9	GD842
40	2.222	7.02	66.3	10.4	GD854

a-Si/a-SiGe/a-SiGe triple-junction solar cells

Incorporating improved doped layers and tunnel junction as well as high quality intrinsic materials, the UT group fabricated triple-junction solar cells [8]. Figure 5 shows a UT a-Si/a-SiGe/a-SiGe triple cell measured at National Renewable Energy Laboratory, showing 11.8% initial, total-area efficiency, which corresponds to a 12.5% initial, active-area efficiency after the coverage by metal contacts is taken into consideration. Figure 6 shows the quantum efficiency curves for top, middle and bottom component cells for the triple cell shown in Fig. 5, exhibiting high spectral response in both blue and red. These triple cells were light soaked under one sun light intensity at 50 C. Figure 6 illustrates the IV curve of a triple cell after 1000 hours of light soaking, showing 10.7% stabilized, active-area efficiency.

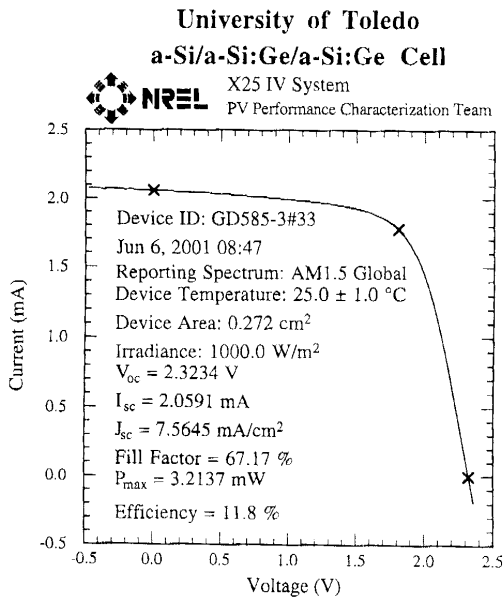


Fig. 5. IV characteristics of a UT fabricated triple cell, measured at NREL, showing 12.5% initial, active-area efficiency (11.8% initial, total-area efficiency).

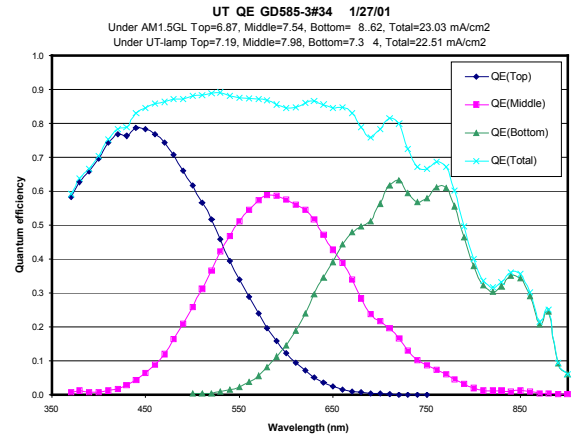


Fig. 6. Quantum efficiency of the 12.5% a-Si/a-SiGe/a-SiGe triple cell.

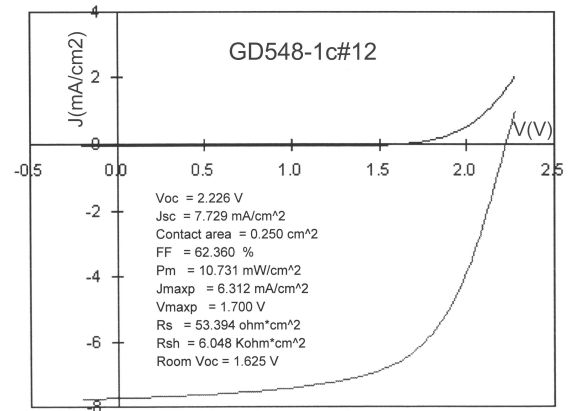


Fig. 7. IV curve of a UT fabricated triple cell after 1000 hours of light soaking under one sun at 50C, showing 10.7% stable efficiency.

a-Si/a-SiGe tandem-junction cells

Using improved doped and undoped layers as well as optimized tunnel junction, a-Si/a-SiGe tandem junction solar cells are also fabricated. The top cell in the tandem is identical to the top cell used in a triple cell while the bottom cell a-SiGe i-layer in the tandem has Ge content between those of the middle and bottom cells in a triple cell. Figure 8 shows an IV curve of a tandem-junction cell, exhibiting 12.9% initial, active-area efficiency [8].

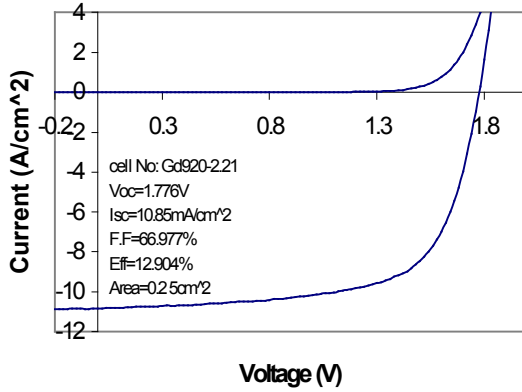


Fig. 8. IV curve of a tandem-junction a-Si/a-SiGe cell, showing 12.9% efficiency.

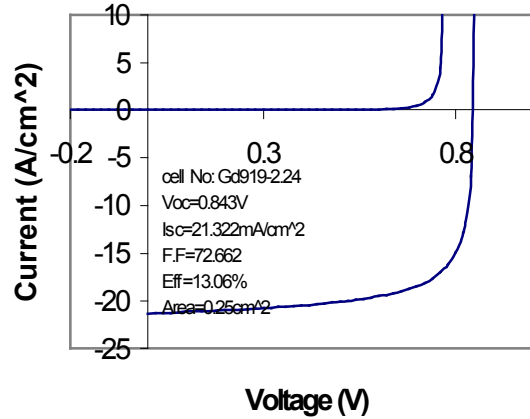


Fig. 9 IV curve of single-junction a-SiGe solar cell, showing 13% initial efficiency.

High efficiency single-junction a-SiGe cells

The high performance nc-Si p-layer deposited at a low temperature (e.g. 70 °C) is found not suitable for a-SiGe i-layer due to a poor match at the band edges between the QCE-enhanced wide bandgap nc-Si p-layer and the reduced bandgap a-SiGe i-layer. However, p-layers deposited at a relatively higher temperature (e.g. 140 °C) exhibit a smaller bandgap, due to reduced QCE when the size of the crystalline grains are increased, and are found to be more suitable (higher FF) for a-SiGe cells. On the other hand, these higher temperature deposited p-layer shows more absorption in the blue due to its reduced bandgap. While these higher absorption in the short wavelength region is not a concern for a multijunction solar cell, in which sunlight is absorbed by the top cell before it reaches the p-layer for a-SiGe cell, such an increased blue absorption results in smaller short circuit current for single-junction a-SiGe cell. A hybrid p-layer, employing two sub-p-layers for the a-SiGe cell is used [10]. In such a hybrid p-layer, a sub-p-layer, ~4nm thick deposited at 70 C, is grown first on the a-SiGe intrinsic layer, to form a good junction, and a second sub-p-layer, ~8nm thick deposited at 140C, is grown on top of the first sub-p-layer. Such a hybrid p-layer is highly transparent, yet forms a high-quality junction with the i-layer. Fig. 9 shows an IV curve of an a-SiGe single-junction cell having an improved p-layer, showing a V_{oc} of 0.843V, J_{sc} of 21.3 mA/cm² and FF of 72.7%, with an initial, active-area efficiency of 13%. The integrated current density from quantum efficiency curves shows a J_{sc} of ~19mA/cm², slightly smaller than the J_{sc} measured in I-V under a solar simulator for this device. The actual efficiency may be between 12-12.5%. Figure 10 shows the IV curves of a similar single-junction a-SiGe cell before and after different light soaking times under one sun at 50C. The cell efficiency is stabilized at ~10.5%.

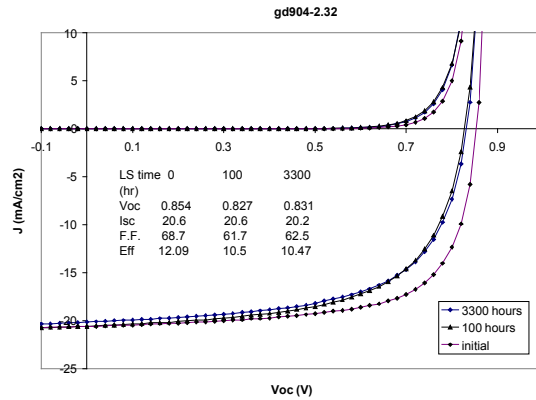


Fig. 10. IV curves of an a-SiGe cell before and after 100 and 3300 hours of one sun light soaking.

Light-assisted electrochemical shunt passivation

An electrochemical process was earlier reported by Nath et al to passivate current-shortening shunts in a-Si based solar cells [23]. A light-assisted electrochemical shunt passivation process was developed at UT [18]. In this process, a schematic of which is shown in Figure 11, a solar cell is placed in an AlCl₃ electrolyte and light is illuminated on the cell which generates a photovoltage. A forward electrical bias is applied on the device. In the area where there is a shunt nearby, the photovoltage is small due to the shunts. The applied electrical bias exerts a voltage at the electrolyte/ITO interface, initiating an electrochemical reduction process that converts ITO near the shunt into an insulator. However, in areas where there is no shunts, the photovoltage would cancel or partially cancel the applied voltage bias, so that the voltage drop at the electrolyte/ITO interface is not sufficient to trigger the ITO reduction. Such a light-assisted electrochemical shunt passivation process is used to effectively remove small

shorts and shunts in a bigger area cell [18]. Figure 12 shows the efficiency of many small test cells on a sample before and after photo-assisted electrochemical shunt passivation. The process recovers most of the shunted cells.

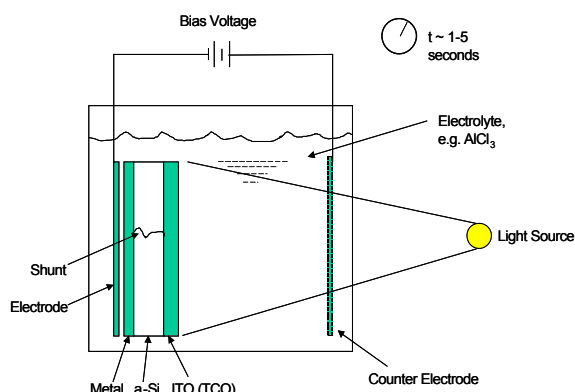


Fig. 11. Schematic of light-assisted electrochemical shunt passivation process.

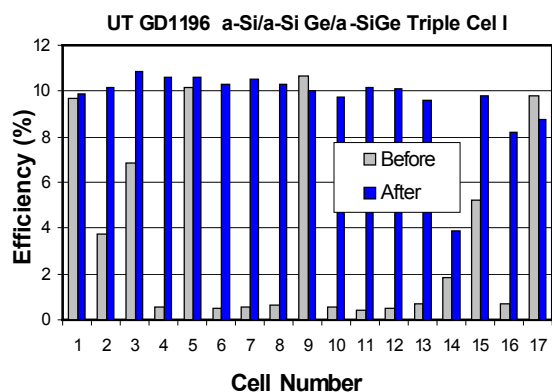


Fig. 12. Efficiency of solar cells before and after shunt passivation, showing the recovery of most of the cells.

Fabrication of submodules

The shunt passivation process described above allows the UT group to fabricate large-area cells and consequently a-Si based photovoltaic submodules [13,14]. Figure 13 shows a 4"x4" and a 4"x8" single-junction a-SiGe submodules encapsulated using silicone elastomer in a UT-built laminator [13].

The UT a-Si group also fabricated triple-junction solar cells on flexible polyimide substrate (Kapton VN) [14]. It is found that the film adhesion is one of the major issues. Further studies reveal that the use of a tie coat, between the polyimide substrate and the metal back-reflector layer, significantly improves the film adhesion [14]. The study shows that chromium, nickel, molybdenum

and zinc oxide can be used as suitable tie coat materials. Using these tie coats and the shunt passivation process described above together with a laser scribing /interconnecting process, the UT group fabricated a-Si/a-SiGe/a-SiGe triple-junction submodules that are lightweight, flexible and monolithically interconnected, as shown in Figure 14.

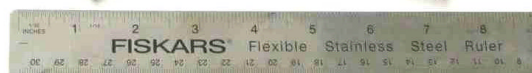


Fig. 13. A photo of two a-SiGe submodules encapsulated with silicone elastomer.

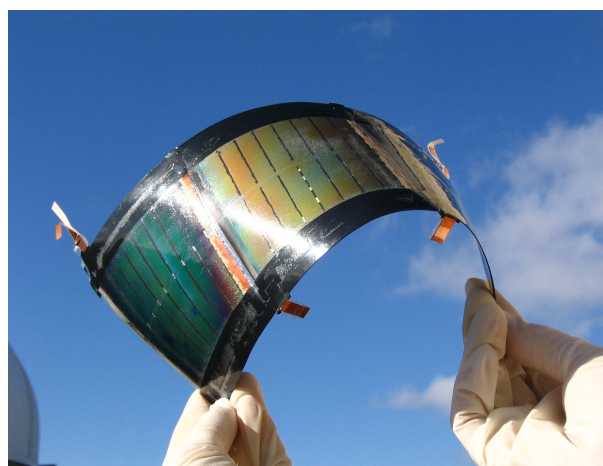


Fig. 14. A photo of a 4"x12" lightweight, flexible, and monolithically interconnected triple-junction a-Si submodule fabricated on polyimide substrate.

SUMMARY

A review of some of the recent research activities at the University of Toledo in a-Si based photovoltaic research is presented. Using improved doped and intrinsic materials, the UT group fabricated high-efficiency triple, tandem and single-junction a-SiGe based solar cells, all with initial active-area efficiency greater than 12.5% and a stabilized efficiency around 10.5%.

ACKNOWLEDGEMENTS

The author is grateful to scientists at Energy Conversion Devices, Inc., United Solar Ovonic Corp., Midwest Optoelectronics, LLC, and the University of Toledo for research collaborations. He is particularly grateful to present and prior members of his research group (Students, Postdocs, Visiting Scholars and Research Technicians) at UT, for carrying out the research covered in this review paper. These members include Pratima Agarwal, Dinesh Attygalle, Koertland Beyer, Xinmin Cao, Chandan Das, Brian Dewhirst, Ashutosh Dighe, Wenhui Du, Lauri Edwards, Sijin Han, Ray Kallaher, Terry Khale, Xianbo Liao, Gregory Miller, Henry Povolny, Joe Sawvel, Dan Sporar, Catherine Taylor, Aarohi Vijh, Jim Walker, Ronghua Wang, Wenjing Wang, Jennifer Wilcox, Xianbi Xiang, Xiesen Yang, and Ramprakash Yerramili. This work is partially supported by National Renewable Energy Laboratory under Thin Film Photovoltaic Partnership Program under subcontract NDJ-2-30630-08 and Air Force Research Lab Space Vehicle Directorate under contract F29601-02-C-0304.

REFERENCES

- [1] M. Izu, X. Deng, A. Krisko, K. Whelan, R. Young, H.C. Ovshinsky, K.L. Narasimhan and S.R. Ovshinsky, "Manufacturing of Triple-junction 4 ft² a-Si alloy PV Modules", Proc. of 23rd IEEE PVSC, 919 (1993).
- [2] S. Guha, J. Yang, A. Banerjee, T. Glaffelter, K. Hoffman, S.R. Ovshinsky, M. Izu, H.C. Ovshinsky and X. Deng, "Amorphous Silicon Alloy Photovoltaic Technology--from R&D to Production", in Proc. of MRS Spring Meeting, 1994, Vol. 336, p.645 (1994).
- [3] X. Deng, M. Izu, K.L. Narasimhan, and S.R. Ovshinsky, in Proc. of MRS Spring Meeting, 1994, Vol. 336, p.699 (1994).
- [4] X. Deng, "Development of High, Stable-efficiency Triple-junction a-Si Alloy Solar Cells", Phase I Annual Subcontract Report, prepared under Subcontract No. ZAN-4-13318-11. (February 1996). NREL/TP-411-20687. Available NTIS: Order No. DE9696000530.
- [5] J. Yang, A. Banerjee, and S. Guha, Appl. Phys. Lett. 70 2975 (1997).
- [6] X. Deng, "Study of triple-junction amorphous silicon alloy solar cells", in American Institute of Physics Conf. Proc. 462, 297 (1998).
- [7] X. Deng and X.B. Liao, S. Han, H. Povolny and P. Agarwal, "Amorphous silicon and silicon germanium materials for high efficiency triple-junction solar cells", Solar Energy Materials & Solar Cells, 62, 89-95 (2000).
- [8] W. Wang, H. Povolny, W. Du, X.B. Liao and X. Deng, "Improved Triple-Junction a-Si Solar Cells with Heavily Doped Thin Interface Layers at the Tunnel Junctions", Proc. of IEEE 29th PVSC, 1082 (2002).
- [9] X. Deng and E. Schiff, "Amorphous Silicon Based Solar Cells", a chapter in The Handbook of Photovoltaic Science and Engineering, ed. A. Luque & S. Hegedus, published by John Wiley & Sons, Ltd. , June, 2003.
- [10] X. Liao, W. Du, X. Yang, H. Povolny, X. Xiang and X. Deng, "High-efficiency single-junction amorphous silicon germanium solar cells", in Proc. 31st IEEE PVSC, 2005.
- [11] W. Du, X. Liao, X. Yang, X. Xiang, X. Deng and K. Sun, "Fine-grained nanocrystalline silicon p-layer for high-Voc a-Si:H solar cells", in Proc. 31st IEEE PVSC, 2005.
- [12] C. Das and X. Deng, "Modeling of triple-junction a-Si solar cells using ASA: Analysis of device performance under various failure scenarios", in Proc. 31st IEEE PVSC, 2005.
- [13] A. Vijh and X. Deng, "Amorphous silicon based minimodules with silicone elastomer encapsulation", in Proc. 31st IEEE PVSC, 2005.
- [14] A. Vijh, X. Yang, W. Du and X. Deng, "Film adhesion in triple-junction a-Si solar cells on polyimide substrates", in Proc. 31st IEEE PVSC, 2005.
- [15] X. Cao, H. Povolny, and X. Deng, "Hot-wire deposition of nanocrystalline SiGe films for thin-film Si based solar cells", in Proc. 31st IEEE PVSC, 2005.
- [16] W. Du, X. Liao, X. Yang, H. Povolny, X. Xiang, X. Deng and K. Sun, "Hydrogenated nonocrystalline silicon p-layer a-Si:H nip solar cells", Submitted to Solar Energy Materials & Solar Cells, 2005.
- [17] C. Das, X. Xiang and X. Deng, "Measurement of component-cell current-voltage characteristics in a double-junction solar cell", to be published in Solar Energy Materials & Solar Cells, 2005.
- [18] A. Vijh and X. Deng, "Light-assisted electrochemical shunt passivation for photovoltaic devices", Patent application submitted to USPTO, April, 2004. Also, A. Vijh and X. Deng, "Light-assisted electrochemical shunt passivation for amorphous silicon photovoltaics", to be submitted to Appl. Phys. Lett. 2005.
- [19] H. Povolny and X. Deng, in Minutes of NREL a-Si team meeting, April 2004, San Francisco, CA.
- [20] X. Deng, "High-efficiency and high-rate deposited amorphous silicon based solar cells", Final Technical Report, 2005, submitted to NREL under Thin Film Partnership Program under subcontract NDJ-2-30630-08. Document also available at <http://www.physics.utoledo.edu/~dengx/papers/papers.htm>
- [21] See Proceedings of 29th and 30th IEEE Photovoltaic Specialist Conference.
- [22] See Proceedings of Materials Research Society Symposium A in 2003 and 2004.
- [23] P. Nath, et al, Appl. Phys. Lett. 53, 11, (1988)